SIMULTANEOUS ESTIMATION OF KINETIC PARAMETERS AND THE INPUT FUNCTION FROM DCE-MRI DATA: THEORY AND SIMULATION

Z. Jane Wang, Zhu Han, K. J. Ray Liu, and Yue Wang[2]

Department of Electrical and Computer Engineering/Institute for Systems Research,
University of Maryland, College Park
[2]Electrical and Computer Engineering Department, Virginia Polytechnic Institute and State University

ABSTRACT

DCE-MRI is a noninvasive functional imaging technique capable of assessing tumor microvasculature clinically. Major limitations associated with conventional region-of-interest (ROI) based compartmental methods include the requirement of invasive acquisition of the input function and labor-intensive identification of the ROIs. We propose a novel blind system identification approach for quantitative imaging by simultaneously estimating the input function and the kinetic parameters. New statistical model is on the pixel domain, whose parameters are initialized using a sub-space based algorithm, and further refined by an iterative maximum likelihood estimation procedure. The performances of the proposed scheme is examined extensively via simulations. The real breast tumor DCE-MRI data are examined by determining the time activity curves and the underlying factor images.

1. INTRODUCTION

Dynamic contrast enhanced magnetic resonance imaging (DCE-MRI) is a noninvasive functional imaging technique, utilizing various molecular weight contrast agents to access tumor microvascular characteristics which provide information about tumor microvessel structures and functions [1].

The region of interest (ROI) based compartmental model analysis is usually used for quantitative dynamic imaging [2]. In such a conventional modelling, the measured concentration of the tracer over time of the tissue within ROI i, referred to as tissue time-activity curve (TAC), is often modelled as the convolution of the regional tissue response $h^{(i)}(t)$ with the tracer concentration in plasma (i.e. the input function) plus the noise, where the tissue impulse response is fully characterized by some kinetic parameters. For instance, as in [2], $h^{(i)}(t) = k_I^{(i)} e^{-k_O^{(i)} t}$, in which the kinetic parameters k_I and k_O represent the washin rate constant and the washout rate constant, respectively. For a single ROI, estimation of the kinetic parameters requires the input function, usually obtained by taking blood samples invasively at the radial artery or from an arterialized vein, which, however, poses health risks and is not compatible with the clinical practice [3]. Therefore, it is of great interest to estimate both the kinetic parameters and input function simultaneously. Only a few works for this purpose have been reported in literature [4]-[7].

However, the ROI-based compartment analysis still suffers from several problems. Briefly speaking, the problem of identifying different ROIs itself remains an essential challenge, and most often we are interested in the underlying heterogeneity characterization. Also, since tumor vascularity may be heterogeneous even at the microscopic level, some degree of intro-voxel heterogeneity is likely [8]. Moreover, clinical observations suggest that multiple biomarkers (e.g. tissue components with different kinetics) affect the tissue impulse response simultaneously. We therefore propose to work on the pixel domain directly while keep the base of compartment modeling. We plan to construct a hybrid approach for estimating the input function and the spatial/temporal patterns of multiple biomarkers simultaneously.

2. SYSTEM MODEL AND FORMULATION

In this paper, without loss of generality, we consider two biomarkers, and focus on the two-compartment model due to its popularity in practical use. However, the schemes developed here can be generalized to cover a more case consisting of multiple biomarkers. Using the two-compartment model [9], we have

$$\begin{aligned} c_f(t) &= k_{1f} a_f(t), \text{ with } a_f(t) = c_p(t) \otimes e^{-k_{2f} t}, \quad (1) \\ c_s(t) &= k_{1s} a_s(t), \text{ with } a_s(t) = c_p(t) \otimes e^{-k_{2s} t}, \end{aligned}$$

where $\otimes$ denotes the convolution operation, $t \geq 0$, $k_{2f} > k_{2s} > 0$, $c_f(t)$ and $c_s(t)$ are the tissue activities in the fast turnover and slow turnover pools, respectively, at time t; $c_p(t)$ is the input function; k_{1f} and k_{1s} are the unidirectional transport constants from plasma to tissues in the fast-flow and slow-flow pools, respectively; k_{2f} and k_{2s} are similarly defined. For pixels $i = 1, ..., N$ within a region, we describe the measured pixel TAC $c_m(i,t)$ as

$$c_m(i,t) = k_{1f}(i) a_f(t) + k_{1s}(i) a_s(t) + v_p(i) c_p(t) + \epsilon(i,t), \quad (2)$$

with $k_{1f}(i)$ and $k_{1s}(i)$ being the local permeability parameters associated with pixel i; $v_p(i)$ means the plasma volume in pixel i; and the noise term $\epsilon(i,t)$. Let $\mathbf{t} = \{t_1, t_2, ..., t_n\}$ indicate the uniform sampling times of the measurements. Let $\mathbf{c}_m(i)$, $\mathbf{a}_f$, $\mathbf{a}_s$, $\mathbf{c}_p$, and $\epsilon(i)$ be the corresponding discrete versions sampled at $\mathbf{t}$. Based on the discrete model, we have

$$\mathbf{a}_f \triangleq \mathbf{H}(k_{2f}) \mathbf{c}_p; \quad \mathbf{a}_s \triangleq \mathbf{H}(k_{2s}) \mathbf{c}_p, \quad (3)$$

where the convolution matrix $\mathbf{H}(k_{2f})$ is Toeplitz determined by $e^{-k_{2f}\mathbf{t}}$. For each pixel i, we have the discrete model

$$\mathbf{c}_m(i) = \mathbf{A}\mathbf{s}(i) + \epsilon(i), \quad (4)$$

with $\mathbf{A} = [\mathbf{a}_f, \mathbf{a}_s, \mathbf{c}_p]$, and $\mathbf{s}(i) = [k_{1f}(i), k_{1s}(i), v_p(i)]^T$.

In our problem, the input $c_p(t)$ also needs to be estimated based on the measurements $c_m(i,t)$'s. Here we consider a parametric model of the input function proposed in [10]. To remove

0-7803-8388-5/04/$20.00

the redundant parameters, we set $a_1 = 1$, and we have the discrete model

$$\mathbf{c}_p = \begin{pmatrix} t_1 e^{\lambda_1 t_1} & e^{\lambda_1 t_1} & e^{\lambda_2 t_1} & e^{\lambda_3 t_1} \\ t_2 e^{\lambda_1 t_2} & e^{\lambda_1 t_2} & e^{\lambda_2 t_2} & e^{\lambda_3 t_2} \\ \vdots & \vdots & \vdots & \vdots \end{pmatrix} \begin{pmatrix} 1 \\ -a_2 - a_3 \\ a_2 \\ a_3 \end{pmatrix} \triangleq \mathbf{B}(\lambda)\mathbf{b} \tag{5}$$

in which $\lambda_1 < \lambda_2 < \lambda_3 < 0$, the vector $\lambda = \{\lambda_1, \lambda_2, \lambda_3\}$, where λ_j's (in min^{-1}) and a_j's (in μCi/ml/min) are the model parameters representing the eigenvalues and the coefficients. Now we note that the signal-matrix $\mathbf{A}$ is fully characterized by parameters k_{2f}, k_{2s},λ_j's, and a_j's, since

$$\mathbf{A} = [\mathbf{H}(k_{2f})\mathbf{B}(\lambda)\mathbf{b}, \mathbf{H}(k_{2s})\mathbf{B}(\lambda)\mathbf{b}, \mathbf{B}(\lambda)\mathbf{b}].$$

We now study the likelihood function of the pixel TAC measurements and formulate the corresponding high-dimensional optimization problem. Assume that the noise $\epsilon(i,t)$ is both temporally and spatially white Gaussian distributed, with zero mean and unknown variance σ^2. Therefore, the complete parameter set is described as $\theta = \{k_{2f}, k_{2s}, \mathbf{c}_p, \mathbf{s}(1), ..., \mathbf{s}(N), \sigma^2\}$ in our problem. Write the whole observations as $\mathbf{X} = [\mathbf{c}_m(1), \mathbf{c}_m(2), ..., \mathbf{c}_m(N)]$, and we can compute the overall likelihood function of $\mathbf{X}$, $f(\mathbf{X};\theta)$. With $\mathbf{A}$ is fixed, the ML estimate of $\mathbf{s}(i)$ and σ^2 can be derived. Substituting the ML estimates of σ^2 and $\mathbf{s}(i)$'s into the overall likelihood, we can show that the ML estimates of θ_s, where $\theta_s = \{k_{2f}, k_{2s}, \lambda_1, \lambda_2, \lambda_3, a_2, a_3\}$, are obtained by solving

$$\hat{\theta}_s = \arg \min_{\theta_s} \text{Tr}\{(\mathbf{I} - \mathbf{A}(\mathbf{A}^T\mathbf{A})^{-1}\mathbf{A}^T)\hat{\mathbf{R}}\} \triangleq \arg \min_{\theta_s} L(\theta_s), \tag{6}$$

with the constraints: $k_{2f} > k_{2s} > 0$ and $\lambda_1 < \lambda_2 < \lambda_3 < 0$, where Tr means the trace operation, $\hat{\mathbf{R}}$ is the sample covariance matrix expressed as $\hat{\mathbf{R}} = \frac{1}{N}\sum_{i=1}^{N} \mathbf{c}_m(i)\mathbf{c}_m(i)^T$. Therefore, our estimation problem is modelled as a high-dimensional optimization problem. Different numerical algorithms can be applied to obtain the ML estimate by solving the above seven-dimensional optimization problem. In this paper, we employ RFSQP (Reduced Feasible Quadratic Programming) algorithm to solve the above constrained nonlinear optimization problem [1], and use the results for comparison.

Based on the estimate of θ_s, we can reconstruct the curves $a_f(t), a_s(t)$ and $c_p(t)$, and it is straightforward to estimate $\mathbf{s}(i)$'s, which represent the factor images revealing the tissue spatial heterogeneity. The high-dimensional numerical approach requires heavy computational cost, and convergence will not always achieve. Therefore, it is of great interest to find an efficient scheme.

3. PROPOSED SCHEME

We propose a scheme consisting of three stages. First, we develop a subspace based algorithm to obtain the initial estimates of the parameters. Secondly, the iterative ML technique is applied to improve the estimation accuracy, where each iteration includes five sub-steps by performing minimization with respect to different sub-sets of parameters. Thirdly, any prior information (belief) will be further evaluated to adjust the estimations.

Sub-space Based Algorithm

Define $\mathbf{f}_0(\alpha)$ be the values of $e^{\alpha t}$ sampled at the uniform sampling time vector $\mathbf{t}$, similarly define $\mathbf{f}_1(\alpha)$ as sampled $te^{\alpha t}$. According to the model in (2), our analysis on Laplace-transform shows that the signal sub-space $\mathbf{S}$ is characterized by exponential decaying signals and the first order derivation of an exponential decaying signal with parameter λ_1, meaning that we have

$$\begin{aligned} \mathbf{c}_m(i) &= [\mathbf{f}_0(-k_{2f}), \mathbf{f}_0(-k_{2s}), \mathbf{f}_0(\lambda_1), \mathbf{f}_1(\lambda_1), \mathbf{f}_0(\lambda_2), \mathbf{f}_0(\lambda_3)]\mathbf{c}(i) \\ &+ \epsilon(i) = \mathbf{S}\mathbf{c}(i) + \epsilon(i), \end{aligned} \tag{7}$$

where the coefficient vector $\mathbf{c}(i)$ indicates the weight of each signal component at pixel i. Now we observe the covariance matrix:

$$\hat{\mathbf{R}} = \mathbf{S}\mathbf{D}\mathbf{S}^T + \sigma^2\mathbf{I}_n = \mathbf{Q}_s\Lambda_s\mathbf{Q}_s^T + \sigma^2\mathbf{Q}_w\mathbf{Q}_w^T, \tag{8}$$

with $\mathbf{D} = E\{\mathbf{c}(i)\mathbf{c}(i)^T\}$, where $\mathbf{Q}_s$ and $\mathbf{Q}_w$ consist of signal and noise eigenvectors, respectively, and the diagonal matrix Λ_s. In our problem, since the signal components represented in $\mathbf{S}$ are coherent as a result of the convolution data model in (2), there is a rank deficiency in matrix $\mathbf{D}$.

A well-known technique to re-store the rank of the signal covariance matrix is the so-called *smoothing* [11]. To achieve the full rank M of $\mathbf{D}$, similarly, we employ the smoothing idea: we split the TACs into a number of overlapping sub-TACs with length n_s; we can show that the signal components in the sub-TACs are identical up to different scalings, and the covariance matrices based on sub-TACs are then averaged. Now, based upon the eigen-structure of $\hat{\mathbf{R}}$, we are particularly interested in one subspace based algorithm, the MUSIC(Multiple SIgnal Classification), because of its wide success in many areas [11]. Therefore, we compute MUSIC-like algorithms as

$$S_0(\alpha) = \frac{1}{\sum_{m=M+1}^{n_s} |\mathbf{q}_m^T\mathbf{f}_0(\alpha)|^2}; \quad S_1(\alpha) = \frac{1}{\sum_{m=M+1}^{n_s} |\mathbf{q}_m^T\mathbf{f}_1(\alpha)|^2} \tag{9}$$

where $0 < e^{\alpha} < 1$, and $\mathbf{q}_m$ are noise eigenvectors. Similar to MUSIC spectrum which exhibits peaks in the vicinity of true frequency components, here the peaks correspond to the exponent parameters of interest (e.g., k_{2f}, k_{2s}, λ_i's). We use the constraints to help the mapping between the peaks and the exponent parameters. Based on the mapping, several sets of the estimates of the exponent parameters can be used as parallel initial estimates. We need to further estimate the coefficients of the input model a_2 and a_3 by minimizing the cost function as defined in (6).

Iterative Likelihood Maximum (ILM)

Since the subspace based method may not always yield sufficient accuracy, we need to fully exploit the underlying data model and apply the ML technique to improve the accuracy. To reduce the computational cost, we propose an iterative alternative, called the iterative likelihood maximization. The main idea is to achieve multidimensional minimization (or maximization) by solving successive lower-dimensional minimization (or maximization) problems iteratively. This idea has its root in the Alternative Maximization (AM) technique [12]. At iteration $(k+1)$, the update of the estimate $\theta_s^{(k+1)}$ is obtained by solving the following one- or two-dimensional minimization problems:

- *Sub-step 1:* Update the ML estimates of the parameter pair (λ_2, a_2), according to the cost function in (6), subject to $\lambda_1^{(k)} < \lambda_2 < \lambda_3^{(k)}$, while all other parameters are held fixed.
- *Sup-step 2:* Update the ML estimates of the parameter pair (λ_3, a_3), with subject to $\lambda_2^{(k+1)} < \lambda_3$.
- *Sub-step 3:* Update the ML estimates of the parameter λ_1, with subject to$\lambda_1 < \lambda_2^{(k+1)}$.
- *Sub-step 4:* Update the ML estimates of the kinetic parameter

[1] For Academic Institutions, the free source code of RFSQP is available from the website http://www.aemdesign.com/.

k_{2f}, with subject to $k_{2f} > k_{2s}^{(k)}$.
- *Sub-step 5:* Updating $\hat{\theta}_s$ accordingly, then update the ML estimates of the kinetic parameter k_{2s}, with subject to $k_{2f}^{(k+1)} > k_{2s}$.

These sub-steps are iteratively applied until the convergence is achieved. Since a minimization is performed at every sub-step, the value of the cost function $L(\theta_s)$ keeps decreasing with the index k. Intuitively, the algorithm reaches the bottom of the cost function $L(\theta_s)$ along lines parallel to the axes.

Further Adjustment

Given that $\mathbf{A}$ is fixed and that the inequality constraints $k_{1f}(i) \geq 0, k_{1s}(i) \geq 0$ and $v_p(i) \geq 0$, for each pixel i, since $\mathbf{c}_m(i)$ follows a $N(\mathbf{A}\mathbf{s}(i), \sigma_2\mathbf{I})$ distribution, estimating the factor coefficients $\mathbf{s}(i)$ equals to solve a constrained optimization problem

$$\hat{\mathbf{s}}(i) = \arg \min_{\mathbf{s}(i)} ||\mathbf{c}_m(i) - \mathbf{A}\mathbf{s}(i)||^2 \text{ subject to } \mathbf{s}(i) \geq 0. \quad (10)$$

The Lagrange multiplier theorem is to solve this problem.

4. SIMULATED DATA RESULTS

The proposed scheme should provide for each parameter an accurate estimate; it should accurately estimate the three factor TACs associated with the extracted from the whole-tumor tissue kinetics (i.e., $a_f(t)$,$a_s(t)$ and $c_p(t)$). As in [5], we consider the coefficient of variation (CV) and the relative bias

$$CV(p) = \frac{std(\hat{p})}{\bar{p}}; \quad bias(p) = |\frac{p - \bar{p}}{p}|, \quad (11)$$

where p represent the true value of the individual parameter, std means standard deviation, $\bar{p}$ is the empirical mean value.

Let $\mathbf{y}$ and $\hat{\mathbf{y}}$ be the true and estimated factor TAC, respectively. To evaluate performance with regard to the objectives, we calculate the correlation coefficient (CC) between the estimated factor TACs $\hat{\mathbf{y}}$ and the true ones $\mathbf{y}$. We also study the norm of the corresponding residuals defined as $(\hat{\mathbf{y}} - \mathbf{y})$, since it is desirable for an estimator to fit the real factor curve in a least-square sense. To make a fair comparison, we perform "centering" and "normalization" on the three factor TACs over time $\mathbf{t}$ before we calculate the above performance measures.

Simulation runs are used to test the accuracy and reliability of the proposed scheme. The input function $c_p(t)$ is generated from the parametric model proposed in [10]. We consider a multi-region significantly-overlapped case. The simulated tumor phantom consists of three underlying components as shown in Fig. 1(a), where a lighter color means a high amplitude. The coefficients (e.g. $\{k_{1f}(i)\}$) are randomly drawn from one of the two uniform distributions: $\{k_{1f}(i)\}$ and $\{k_{1s}(i)\}$ are from the uniform distributions $U(0.1, 0.4)$ and $U(0.8, 1)$, and $\{v_p(i)\}$ are from $U(0.2, 0.3)$ and $U(0.4, 0.8)$. The TACs are sampled from 0 to 10 minutes with the uniform sampling period 15 seconds. The noise level is chosen as $\sigma^2 = 30$ to yield a similar SNR observed in real image data.

Based on 100 simulations runs, we study the performance measures discussed above. Table 1 shows the statistical results of estimating the kinetic parameters. It is worth mentioning that the computational complexity of the proposed scheme is much lower than that of RFSQP. As mentioned earlier, we only report the estimate of the ratios a_2/a_1 and a_3/a_1 to avoid the redundant parameter. Within each cell of the table, we report the corresponding result of RFSQP before the sign | and that of the proposed scheme after the sign |. For instance, 0.266|0.227 means that the relative bias 0.266 of k_{2f} obtained from the RFSQP algorithm is 0.266, which it is 0.277 from the proposed scheme. From this table, we can see that the resulting CVs and relative biases are reasonably small. Overall the proposed scheme provides comparable performance in estimating parameters, compared with RFSQP. However, it is worth mentioning that the accuracy in estimating individual parameter is of less importance in our problem. We are more interested in identifying different signal components and find out their space patterns within a tumor region.

For each factor TAC, we study the resulting correlation coefficient and the residual norm. Their empirical means and standard deviations are shown in Table 2. We note that the proposed scheme provides a little worse but very close performance to that of RFSQP. An interesting observation is that both schemes works well in estimating the slow-flow factor curve $a_s(t)$, although it was noted earlier that the proposed scheme works much worse in estimating the kinetic parameter k_{2s}. It can be seen that the proposed scheme provides high accuracy in estimating the curves $a_f(t)$,$a_s(t)$ and $c_p(t)$ which characterize the underlying components in this tumor phantom case.

We are particularly interested in estimating the factor images. One example is shown in Fig. 1. It can be seen that the proposed scheme provides high accuracy in estimating the factor images which demonstrate the spatial heterogeneity of each component.

5. REAL DATA RESULTS

We now examine the DCE-MRI study of breast cancer patients. The data was acquired at NIH laboratory, where the Gadolinium DTPA was used as the contrast agent, and 3D scans of DCE-MRI were performed every 30 seconds for a total of 11 minutes after the injection. Fig. 2(a) shows the input function estimated by the proposed scheme. In addition, we also plot the estimated factor curves for the fast-flow and the slow flow. The factor TACs follow compartmental kinetics and their shapes are what we expect. To further examine the results, based on the above estimate of the parameters, we reconstruct the factor images (i.e. $\mathbf{s}(i)$'s) in Fig. 2(b). It is noted that the boundary region is dominated by the fast flow, while the inside region is dominated by the slow flow. Meanwhile, the input signal component is observed everywhere in some sense, with stronger energy around edges. The observations match with the clinical opinions. The fast slow parameters on the left of tumor area are more active than those of the other parts. Future work will involve studies with a microsphere based gold standard of flow to validate the proposed scheme.

6. CONCLUSION

The goal of this research is to develop efficient methods for characterizing multiple biomarkers and estimating the input function in dynamic imaging. We investigated the system model on the pixel domain consisting of multiple biomarkers, and developed an integrated scheme including iterative steps to estimate the kinetic parameters and the input function simultaneously. Based on several performance measures, the simulation results illustrated that the proposed scheme is able to quantify all the unknown parameters, provides reliable estimations of factor TACs, and proves very promising in examining the spatial heterogeneity in tissue dynamics on pixel-by-pixel basis. Furthermore, we studied the result on brain PET, where the results clearly reveal the spatial heterogeneity in tumor structure which matches with the clinical belief.

parameter p	k_{2f}	k_{2s}	λ_1	λ_2	λ_3	a_2/a_1	a_3/a_1
true value	2.5	0.4	-4.1339	-0.2191	-0.0104	0.0257	0.0245
$bias(p)$	0.266|0.227	0.196|0.607	0.122|0.012	0.302|0.326	2.128|2.663	0.062|0.013	1.618|1.856
$CV(p)$	0.138|0.229	0.179|0.188	-0.061|-0.107	-0.299|-0.829	-0.201|-0.284	0.312|1.336	0.381|0.312

Table 1. Estimation performance of the parameters for the noise level $\sigma^2 = 30$, based on 100 simulation runs.

factor TAC	$a_f(t)$	$a_s(t)$	$c_p(t)$
CC	(0.973,0.079)|(0.935,0.085)	(0.995,0.003)|(0.996,0.009)	(0.973,0.025)|(0.951,0.0442)
residual norm	(0.053,0.159)|(0.13,0.171)	(0.010,0.006)|(0.0082,0.0179)	(0.053,0.049)| (0.0975,0.0884)

Table 2. Performance of estimating the factor TACs $a_f(t), a_s(t)$ and $c_p(t)$. The mean and standard deviation are calculated.

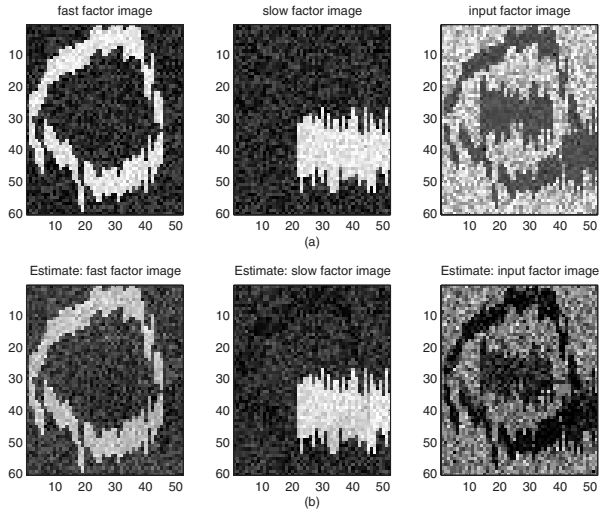

Fig. 1. Factor images in the simulated tumor phantom. (a) the true factor images; and (b) the estimated factor images.

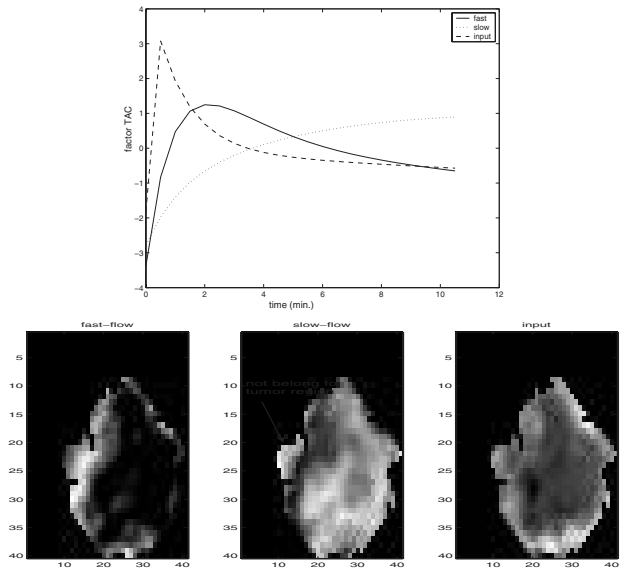

Fig. 2. (Upper) The factor TACs estimated by the proposed scheme on real breast cancer data. (Lower) The estimated factor images in the breast tumor after applying the proposed scheme.

7. REFERENCES

[1] M. Neeman, J. Provenzale, M. Dewhirst, "Magnetic Resonance Imaging Applications in the Evaluation of Tumor Angiogenesis", *Simin. Radiat Oncol 11*, pp. 70-82, 2001.

[2] J. Vallee, H. Sostman, J. MacFall, T. Wheeler, L. Hedlund, C. Spritzer, and R. Coleman,"MRI Quantitative Myocardial Perfusion with Compartmental Analysis: A Rest and Stress Study", *Magn. Reson. Med.*, vol. 38, pp. 981-989, 1997.

[3] J. Correia,"Editorial: A Bloody Future for Clinical PET", *Journal of Nucl. Med.*, vol. 33, pp. 620-622, 1992.

[4] K. Wong, D. Feng, S. Meikle, and M. Fulham, "Simultaneous Estimation of Physiological Parameters and Input Function - In vivo PET Data", *IEEE Trans. Inform. Tech. Biomed.*, vol. 5, pp. 67-76, Mar. 2001.

[5] D. Feng, K. Wong, C. Wu, and W. Siu, "A Technique for Extracting Physiological Parameters and the Required Input Function Simultaneously from PET Image Measurements: Theory and Simulation Study", *IEEE Trans. Inform. Tech. Biomed.*, vol. 1, pp. 243-254, Dec. 1997.

[6] K. Wong, R. Meikle, D. Feng, and M. Fulham, "Estimation of Input Function and Kinetic Parameters Using Simulated Annealing: Application in a Flow Model", *IEEE Trans. On Nuclear Science*, vol. 49, no. 3, June 2003.

[7] D. Riabkov and E. Bella, "Estimation of Kinetic Parameters Without Input Functions: Analysis of Three Methods for Multichannel Blind Identification", *IEEE Trans. on Biomedical Eng.*, vol. 49, no. 11, Nov. 2002.

[8] G. M. Tozer, S. Lewis, A. Michalowaski, V. Aber,"The Relationship between Regional Variations in Blood Flow and Histology in A Transplanted Rat Fibrosarcoma, *Br. J. Cancer*, vol. 61, pp. 250-257, 1990.

[9] Y. Zhou, S-C Huang, T. Cloughesy, C. K. Hoh, K. Black, and M. E. Phelps, "A Modeling-Based Factor Extraction Method for Determining Spatial Heterogeneity of Ga-68 EDTA Kinetics in Brain Tumors", *IEEE Trans. Nuclear Sci.*, vol. 44, no. 6, pp. 2522-2527, Dec. 1997.

[10] D. Feng, S. Huang, and X. Wang,"Models for Computer Simulation Studies of Input Functions for Tracer Kinetic Modeling with Positron Emission Tomography", *Int. J. Biomed. Comput.*, vol. 32, pp. 95-110, 1993.

[11] H. Krim and M. Viberg, "Two Decades of Array Signal Processing Research", *IEEE Signal Processing Magazine*, pp. 67-93, July 1996.

[12] I. Ziskind and M. Wax, "Maximum Likelihood Localization of Multiple Source by Alternate Projection", *IEEE Trans. ASSP*, vol. 36, pp. 1553–1560, Oct. 1988.